



# Methoxyeugenol Protects Against Lung Inflammation and Suppresses Neutrophil Extracellular Trap Formation in an LPS-Induced Acute Lung Injury Model

Géssica Luana Antunes<sup>1,4</sup> , Lucas Strassburger Matzenbacher<sup>1</sup>, Bruna Pasqualotto Costa<sup>1</sup>, Bruno de Sousa Basso<sup>1</sup>, Vitor Giancarlo Schneider Levorse<sup>1</sup>, Krist Helen Antunes<sup>2</sup>, Zaquer Suzana Munhoz Costa-Ferro<sup>3</sup> and Jarbas Rodrigues de Oliveira<sup>1</sup>

Received 16 October 2021; accepted 26 January 2022

**Abstract**— Acute lung injury (ALI) is a life-threatening acute inflammatory disease with high rates of morbidity and mortality worldwide. 4-Allyl-2,6-dimethoxyphenol (methoxyeugenol), a phenylpropanoid from a synthetic source, exhibits strong anti-inflammatory activity, but its effects on the inflammation of ALI have not yet been reported. In our study, the anti-inflammatory effects of methoxyeugenol were investigated on RAW 264.7 cells and a mice model of ALI. Our results showed that methoxyeugenol (7.5 and 30  $\mu$ M) attenuated the proliferation and gene expression of interleukin (IL)-6 in LPS-stimulated RAW 264.7 cells. In a mice model of ALI induced with LPS, methoxyeugenol exhibited a significant protective effect, based on influx reduction of macrophages and neutrophils into the lungs; reduction in release of the cytokines IL-6, TNF- $\alpha$ , and IL-10; and in reactive oxygen species (ROS) formation. We show that the anti-inflammatory effects of methoxyeugenol are associated with the suppression of the NF $\kappa$ B signaling pathway. Moreover, we demonstrated for the first time that a phenolic compound, from a synthetic source, protects against lung tissue inflammation and promotes a reduction of NET formation. These findings provided evidence for the use of methoxyeugenol as a new strategy to control inflammation in ALI disease.

**KEY WORDS:** methoxyeugenol; acute lung injury; inflammation; neutrophil extracellular trap

<sup>1</sup>Laboratory of Cellular Biophysics and Inflammation, Pontifical Catholic University of Rio Grande Do Sul (PUCRS), 6690 Ipiranga Ave, Porto Alegre, RS 90610-000, Brazil

<sup>2</sup>Laboratory of Clinical and Experimental Immunology, Pontifical Catholic University of Rio Grande Do Sul (PUCRS), Porto Alegre, Brazil

<sup>3</sup>Brain Institute of Rio Grande Do Sul (BraIns), Pontifical Catholic University of Rio Grande Do Sul (PUCRS), Porto Alegre, RS, Brazil

<sup>4</sup>To whom correspondence should be addressed at Laboratory of Cellular Biophysics and Inflammation, Pontifical Catholic University of Rio Grande Do Sul (PUCRS), 6690 Ipiranga Ave, Porto Alegre, RS, 90610-000, Brazil. Email: gessica.antunes@edu.pucrs.br

## INTRODUCTION

Acute lung injury (ALI) is characterized by acute respiratory failure, which has a high rate of in-hospital mortality [1]. The treatment for ALI involves mechanical ventilation and pharmacological therapy. However, the pharmacological therapy used has a small effect on patient mortality [2]. Thus, ALI lacks proper therapeutic medicine. During lung injury, resident macrophages are activated and secrete cytokines, starting the inflammation process. Subsequently, neutrophils are recruited into the lung parenchyma and alveolar space and then contribute to lung inflammation through cytokine release, reactive oxygen species (ROS) production, and excessive formation of neutrophil extracellular traps (NETs) [3–5]. NETs are structures formed by DNA strands that are associated with proteins, such as myeloperoxidase (MPO) [5]. The production of NETs was detected in bronchial aspirates from patients with an acute respiratory infection, aggravating lung injury [6].

Natural compounds obtained from plants as crude extracts or isolated molecules have been used for the treatment of several diseases. Particularly, the use of phenolic compounds has aroused great interest due to their therapeutic effects. The phenolic compounds are found in plants, such as *Myristica fragrans* (an herb known as nutmeg) [7]. Studies with nutmeg extract showed anti-inflammatory effects, and the use of chromatographic techniques revealed the presence of methoxyeugenol in the composition of the extract [7–9]. Interestingly, our previous research reported that 4-allyl-2,6-dimethoxyphenol (methoxyeugenol), from a synthetic source, at 30  $\mu\text{M}$  decreased the proliferative rate and induced a quiescent phenotype in the hepatic stellate cells. This same study showed that methoxyeugenol at 0.25 mg/kg attenuated the inflammatory profile and fibrosis in mice submitted to the model of liver fibrosis [10]. Thus, the promising anti-inflammatory activity of methoxyeugenol drew attention as a potential therapeutic agent for ALI. In our study, the anti-inflammatory effects of methoxyeugenol were researched on LPS-stimulated RAW 264.7 cells and mice model of LPS-induced ALI.

### Methoxyeugenol

Was acquired from Sigma-Aldrich, USA (Cat. W365505/Lot.STBD5682V).

## METHODS

### RAW 264.7 Cell Culture

A murine macrophage cell line, RAW 264.7 cells, was purchased from American Type Culture Collection (ATCC TIB-71, USA). DMEM supplemented with 10% fetal bovine serum (FBS) and 1% streptomycin/penicillin antibiotics (ATB) (Gibco, Life-technologies, USA) were used for cultivation of RAW 264.7 cells. RAW 264.7 cells were cultured at 37 °C in a humidified incubator containing 5% CO<sub>2</sub>. Upon reaching a growth corresponding to 80% of confluence, experiments with RAW 264.7 cells were performed.

### Methoxyeugenol Pretreatment and Stimulation with LPS in the RAW 264.7 Cells

Methoxyeugenol (Sigma-Aldrich, USA) was diluted in DMEM 0.5% dimethylsulfoxide (DMSO) (Neon, Brazil) at 1.87, 7.5, and 30  $\mu\text{M}$ . The RAW 264.7 cells were pretreated with methoxyeugenol at 1.87, 7.5, and 30  $\mu\text{M}$  for 1 h before stimulation with LPS (1  $\mu\text{g}/\text{mL}$ ) (Sigma-Aldrich, USA).

### 3-(4,5-Dimethylthiazol-2-yl)-2,5-Diphenyltetrazolium Bromide (MTT) Assay

The plate containing the solution with MTT in all wells was incubated at 37 °C for 3 h. After that, the MTT solution was discarded, and DMSO was added to all wells to dissolve the formazan crystals. The absorbance was measured at 570 nm using a microplate reader (EZ Read 400; Biochrom). A digital DP73 camera coupled to a BX43 light microscope (Olympus, Japan) was used to capture the representative images of the wells.

### Animals

The male adult BALB/cByJ mice used in our study were provided by the Center for Experimental Biological Models (CeMBE, Brazil) of the PUCRS. The BALB/cByJ mice were housed according to standard conditions at 23  $\pm$  2 °C a 12 h/12 h light/dark cycle and with free access to water and food. All experiments were performed following the National Institutes of Health Guide for the

Care and Use of Laboratory Animals. The study and all experiments were approved by the Animal Ethics Committee of the PUCRS with registration number 9607.

### **Methoxyeugenol Pretreatment and LPS-Induced ALI Model**

The mice were randomly divided into the following three groups:

1. Sham group: mice were anesthetized by inhaling isoflurane and intranasal PBS was administered. Then, the mice were immediately treated with DMSO (vehicle) intraperitoneally;
2. LPS-induced ALI group: mice were anesthetized by inhaling isoflurane and intranasal LPS (2 mg/kg in PBS) was administered to induce ALI. Then, the mice were immediately treated with DMSO (vehicle) intraperitoneally;
3. Methoxyeugenol + LPS-induced ALI group: mice were anesthetized by inhaling isoflurane and intranasal LPS (2 mg/kg in PBS) was administered to induce ALI. Then, the mice were immediately treated with methoxyeugenol (0.25 mg/kg in DMSO). The dose of 0.25 mg/kg is based on the previous research [10].

Twelve hours after ALI induction, the mice were anesthetized with ketamine and xylazine (0.4 mg/g and 0.2 mg/g, respectively) and killed by exsanguination via cardiac puncture. The samples of bronchoalveolar lavage (BAL) and lung tissue were obtained.

### **BAL Collection**

The BAL was collected by two consecutive flushes with PBS (1 mL) containing 2% FBS in the lung through a tracheal cannula. The BAL was centrifuged (420 g, 5 min, 4 °C). The cell-free supernatant was used for the quantification of extracellular DNA. The cell pellet was resuspended with 350 µL of PBS at 2% FBS for analysis of cellularity.

### **Cellularity of BAL**

The trypan blue exclusion assay was performed to verify the total cell counts (TCC). The slides of differential cytology were performed according to the method described previously [11]. A digital DP73 camera coupled

to a BX43 light microscope (Olympus, Japan) was used to capture the representative images of differential cytology.

### **Histopathological Analysis**

The lung tissue was perfused by buffered formalin, collected, and embedded in paraffin. Thereafter, slices were cut at 4 µm and stained by H&E (Cytological Products, Brazil). The histopathological changes of lung tissues were evaluated using a semi-quantitative scoring method [12]. Briefly, histological criteria were assigned blindly for the severity scoring of lung inflammation that included interstitial inflammation, inflammatory cell infiltration, congestion, and edema. The histopathological scores were graded from 0 (normal) to 4 (severe) and were obtained by averaging the scores attributed to the individual mice in each group. A digital DP73 camera coupled to a BX43 light microscope (Olympus, Japan) was used to capture the representative images of the lung sections.

### **Immunofluorescence of NFκB p65**

The RAW 264.7 cells or lung sections were fixed and permeabilized with 4% paraformaldehyde (Sigma Aldrich, USA) and 0.1% Triton X-100 (Sigma Aldrich, USA), respectively, for 15 min. Then, the samples were blocked with bovine serum albumin (BSA) at 1% for 20 min and incubated at 4 °C overnight with anti-NFκB p65 (1:500) (Cell Signaling Technology, USA) and then incubated with donkey anti-rabbit IgG conjugated with FITC (1:500) (Thermo Fisher Scientific, USA) for 60 min. 4,6-Diamidino-2-phenylindole (DAPI) (Sigma-Aldrich, USA) at 1 mg/mL for 5 min was used to stain the cellular nuclei. A digital DP73 camera coupled to a BX43 fluorescence microscope (Olympus, Japan) was used to capture all images.

### **Western Blot**

Cells from the lung tissue were lysed using a specific buffer at 12,000 g for 30 min at 4 °C. Total protein concentration was determined by a NanoDrop Lite spectrophotometer (Thermo Scientific, USA). Equal amounts of protein (30 µg) were separated on electrophoresis (SDS-PAGE) and then transferred to a nitrocellulose membrane (Bio-Rad, USA). Membranes

were blocked for 30 min with BSA at 5% and incubated at 4 °C overnight with the following primary antibodies: anti-NFκB p65 (1:500) (Cell Signaling, Danvers), anti-NFκB p-p65 (1:250) (Cell Signaling, Danvers), and anti-β actin (1:1000) (Thermo Fisher Scientific, USA). Afterwards, the blot was incubated with the secondary antibody anti-IgG (1:2000) (Thermo Fisher Scientific, USA) for 2 h. An enhanced chemiluminescence (ECL) system was used for visualizing all protein bands, and quantification was performed using ImageJ software.

### RNA Extraction and RT-qPCR

The RNA from RAW 264.7 cells or lung tissues was extracted using TRIzol. All samples had the total RNA concentration normalized at 5 μg, and a corresponding cDNA library was constructed. Then, the samples were subjected to RT-qPCR using the following primers: TNF-α (forward primer: 5'-ATAGCTCCCAGAAAAGCAAGC'-3, reverse primer: 5'-CACCCCGAAGTTCAGTAGACA-3'), IL-6 (forward primer: 5'-TGGAGTCACAGAAGGAGTGGC TAAG-3', reverse primer: 5'-CTGACCACAGTGAGG AATGTCCAC-3'), IL-10 (forward primer: GCCAAG CCTTATCGGAAATG, reverse primer: AAATCACTC TTCACCTGCTCC), and beta-2-microglobulin (B2M) (forward primer: 5'-CCCCAGTGAGACTGATACATACG-3', reverse primer: 5'-CGATCCAGTAGACGGTCTTG-3'). SYBR Green (Applied Biosystems, USA) was used to catalyze the PCR reaction. The relative expression of B2M mRNA levels was quantified by RT-qPCR, using the StepOne™ Real-Time PCR System (Applied Biosystems, USA). The relative amounts of these mRNAs were determined using the comparative delta-delta Ct method ( $\Delta\Delta Ct$ ).

### Measurement of Cytokines

The total lung tissues were collected and homogenized with PBS solution. ProcartaPlex (Thermo Fisher Scientific, USA) was used to simultaneously measure IL-6, TNF-α, IL-1β, and IL-10. MagPix (MILLIPIX®) equipment and xPONENT® 4.2 (MILLIPIX®) software were used to evaluate the data. The graphics show picograms (pg) of cytokines/mg of total protein.

### ROS Measurement

Total lung tissues were homogenized in the PBS solution, and the supernatants were incubated with a

solution of 2',7'-dichlorofluorescein diacetate (H2DCF-DA) at 100 μM. The incubation generated a fluorescent compound, dichlorofluorescein (DCF), that was measured at  $\lambda_{em} = 488$  nm and  $\lambda_{ex} = 525$  nm [13]. The graphics show DCF fluorescence/mg protein.

### DNA Quantification

The extracellular DNA present on the supernatant of the BAL was quantified using the Qubit 2.0 fluorimeter (Invitrogen, USA) and the Quant-iT dsDNA HS Kit (Invitrogen, USA).

### Immunofluorescence in BAL Cells

To visualize the formation of NETs, BAL cells were seeded in 8-chamber culture slides and incubated at 37 °C with 5% CO<sub>2</sub>. After 1 h of incubation, the cells were stimulated for another hour with 50 nM phorbol myristate acetate (PMA). Subsequently, cells were incubated with paraformaldehyde at 4% (Sigma-Aldrich, USA) for 45 min; then, the fixed cells were incubated with anti-MPO (1:250) (Cell Signaling Technology, USA). After 45 min, cells were incubated with donkey anti-rabbit IgG conjugated with FITC (1:500) (Thermo Fisher Scientific, USA) for 60 min. Finally, the cells were stained with DAPI (1:2000) (Invitrogen, USA) for 4 min. A digital DP73 camera coupled to a BX43 fluorescence microscope (Olympus, Japan) was used to capture all images.

### Scanning Electron Microscopy in BAL Cells

The coverslips treated with poly-L-lysine (Sigma-Aldrich, USA) at 0.0005% were used to seed the BAL cells. The cells were incubated at 37 °C with 5% CO<sub>2</sub>, and after 1 h, the cells were stimulated for another hour with PMA (50 nM). Next, the BAL cells were fixed by glutaraldehyde 2.5% for 7 days. Then, osmium tetroxide solution at 2% was used to postfix the neutrophils for 45 min. Next, the BAL cells were dehydrated using graded acetone. The CO<sub>2</sub> was used to execute the critical point technique and then mounting on a metallic support using carbon tape was performed. Gold was used to cover all samples, and images were captured by Inspect F50 (FEI, Oregon, EUA).

### Cell Death in BAL Cells

Cell death on BAL cells was assessed using annexin V to verify apoptosis and propidium iodide (PI) to verify

necrosis. Cell death on BAL was evaluated by FACS Canto II and FlowJo software (BD Bioscience).

## Statistical Analysis

GraphPad Prism 8 software (GraphPad Software, CA) was used to perform all statistical analyses. Data are expressed as mean  $\pm$  SEM and analyzed by one-way ANOVA, followed by Tukey's post-test. A  $p$  value  $< 0.05$  was considered statistically significant.

## RESULTS

### Methoxyeugenol Decreases LPS-induced Cell Proliferation without a Change in the Viability of RAW 264.7 Cells

Initially, we checked the effect of methoxyeugenol on the viability of RAW 264.7 cells. Cells were pretreated for 24 h with three concentrations of methoxyeugenol (1.87, 7.5, and 30  $\mu$ M), and cytotoxicity was evaluated through the MTT assay. Our data shows that methoxyeugenol did not alter the viability of RAW 264.7 cells (Fig. 1A).

The RAW 264.7 cells were pretreated with methoxyeugenol at 1.87, 7.5, and 30  $\mu$ M for 1 h, followed by stimulation with LPS at 1  $\mu$ g/mL. LPS significantly induced the proliferation of RAW 264.7 cells (Fig. 1B, C). On the other hand, the three tested concentrations of methoxyeugenol decreased the proliferation of RAW 264.7 cells (Fig. 1B, C).

### Methoxyeugenol Reduces mRNA Expression of IL-6 in LPS-stimulated RAW 264.7 Cells

LPS is known to activate the NF $\kappa$ B signaling pathway, which promotes the transcription and expression of inflammatory mediators, such as cytokines. The RAW 264.7 cells were pretreated with methoxyeugenol (1.87, 7.5, and 30  $\mu$ M), and after 1 h of treatment, 1  $\mu$ g/mL of LPS was added to the cells. After 1 h of stimulation with LPS, the shift of NF $\kappa$ B p65 to the nucleus in RAW 264.7 cells was analyzed using immunofluorescence staining. The immunofluorescence images indicated a nuclear accumulation of NF $\kappa$ B p65 after stimulating RAW 264.7 cells with LPS (Fig. 2A). However, nuclear translocation of NF $\kappa$ B p65 was not indicated in the RAW 264.7 cells after pretreatment with methoxyeugenol at 7.5 and 30  $\mu$ M (Fig. 2A).

Additionally, mRNA levels of pro-inflammatory genes were assessed by quantitative RT-PCR. RAW 264.7 cells were pretreated with methoxyeugenol (1.87, 7.5, and 30  $\mu$ M) for 1 h and then stimulated with 1  $\mu$ g/mL of LPS. After 16 h of stimulation with LPS, the samples were collected and RT-qPCR was performed. Our data revealed that TNF- $\alpha$  mRNA expression was not altered between the studied groups (Fig. 2B). On the other hand, the level of IL-6 mRNA was increased in LPS-stimulated RAW 264.7 cells (Fig. 2C). However, the RT-qPCR results revealed that cells pretreated with methoxyeugenol at concentrations of 7.5 and 30  $\mu$ M had a decrease in IL-6 mRNA expression (Fig. 2C).

These experiments showed that methoxyeugenol (7.5 and 30  $\mu$ M) has anti-inflammatory activity in LPS-stimulated RAW 264.7 cells. The ability of methoxyeugenol to promote an anti-inflammatory environment was also explored using an in vivo model. LPS-induced ALI mice were pretreated with 0.25 mg/kg of methoxyeugenol. This concentration was selected because in a study with methoxyeugenol performed by our research group, the concentration at 0.25 mg/kg showed more potent anti-inflammatory effects [10] due to its equivalence to the concentration used in RAW 264.7 cells. Also, it was reported as being a safe dose by the European Food Safety Authority [14].

### Methoxyeugenol Decreases the Influx of Macrophages and Neutrophils into the Lung in LPS-induced ALI Mice

To evaluate the effects of methoxyeugenol in the influx of inflammatory cells, we performed the total cell counts (TCC) in the BAL of mice. As expected, the LPS-induced ALI mice showed an increase in TCC as compared to the sham group (Fig. 3A). However, the influx of cells was decreased in the LPS-induced ALI mice pretreated with methoxyeugenol (Fig. 3A). The differential cell counts revealed that LPS-induced ALI mice had a significant rise in the counts of macrophages and neutrophils, but were notably decreased by pretreatment with methoxyeugenol (Fig. 3B–D). The histopathological analysis also indicated that methoxyeugenol decreased the massive influx of macrophages and mainly of neutrophils. Furthermore, H&E staining was used to evaluate the histopathological changes. The sham group indicated no histopathologic alteration in the lung tissues. However, interstitial inflammation, inflammatory cell infiltration, congestion, and edema were observed in LPS-induced ALI mice. On the other hand, pretreatment with methoxyeugenol ameliorated histopathological changes (Fig. 3E, F).



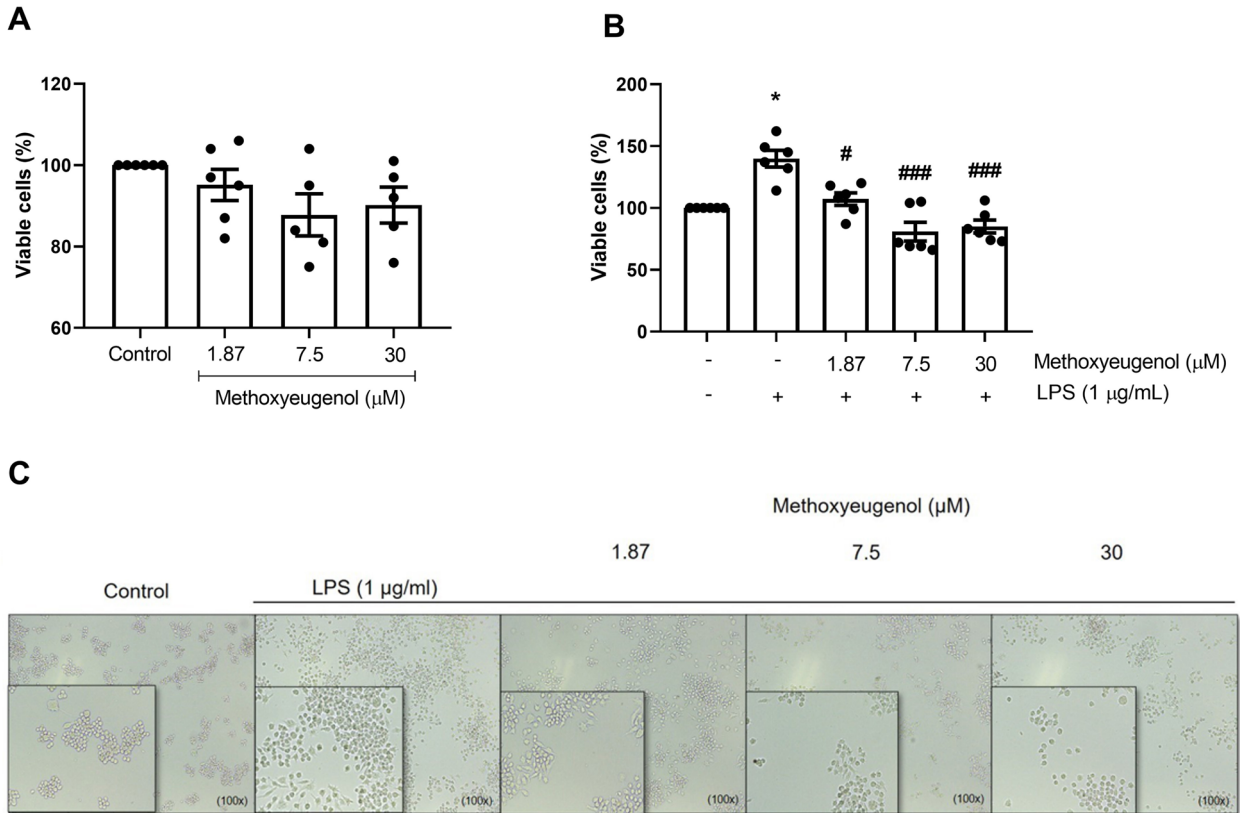


**Fig. 1** Methoxyeugenol does not change the viability of RAW 264.7 cells and decreases LPS-induced proliferation. **A** RAW 264.7 cells ( $1 \times 10^4$  cells/well in 24-well plates) pretreated for 24 h with methoxyeugenol at concentrations of 1.87, 7.5, and 30  $\mu\text{M}$ . **B** RAW 264.7 cells ( $1 \times 10^4$  cells/well in 24-well plates) pretreated for 1 h with methoxyeugenol at concentrations of 1.87, 7.5, and 30  $\mu\text{M}$  and then exposed to LPS (1  $\mu\text{g}/\text{mL}$ ) for 24 h. **C** Representative images of the respective wells. \* Significant difference relative to control; # significant difference relative to LPS (one-way ANOVA followed by Tukey's test) \* $p < 0.05$ , \*\* $p < 0.01$ , and \*\*\* $p < 0.001$ . Results are expressed as viable cells (%), and the data represent the mean  $\pm$  SEM from three independent experiments.

### Methoxyeugenol Regulates the NF $\kappa$ B Signaling Pathway and Decreases the Release of Cytokines in LPS-induced ALI Mice

The effects of methoxyeugenol on the NF $\kappa$ B p65 signaling pathway in the lung tissues of mice were investigated through immunofluorescence staining. As shown in Fig. 4A, the immunofluorescence images indicated that the expression of NF $\kappa$ B p65 in ALI mice was elevated compared with sham mice, whereas it was reversed by pretreatment with methoxyeugenol (Fig. 4A). Furthermore, we determined the protein expression of NF $\kappa$ B p65 and phosphorylated NF $\kappa$ B (p-p65) levels by Western blot. The results showed that the relative expression of p-p65/p65 was increased in ALI mice when compared with sham mice (Fig. 4B). On the other hand, mice pretreated

with methoxyeugenol showed a decrease in the relative expression of p-p65/p65 (Fig. 4B). Our data demonstrate that the effects of methoxyeugenol are associated with the suppression of the NF $\kappa$ B signaling pathway.

To evaluate the production of cytokines, we investigated the gene expressions of TNF- $\alpha$ , IL-6, and IL-10 in the lung tissue of mice by RT-qPCR. TNF- $\alpha$  and IL-6 mRNA expression significantly increased the release in the LPS-induced ALI mice, whereas mice pretreated with methoxyeugenol decreased their expression (Fig. 4C, D). IL-10 mRNA expression did not differ between the studied groups (Fig. 4E). Furthermore, the levels of IL-1 $\beta$ , TNF- $\alpha$ , IL-6, and IL-10 in the lung tissue were evaluated by a Multiplex Assay Kit. The IL-1 $\beta$  levels had increased in LPS-induced ALI mice; however, treatment with methoxyeugenol did not reduce

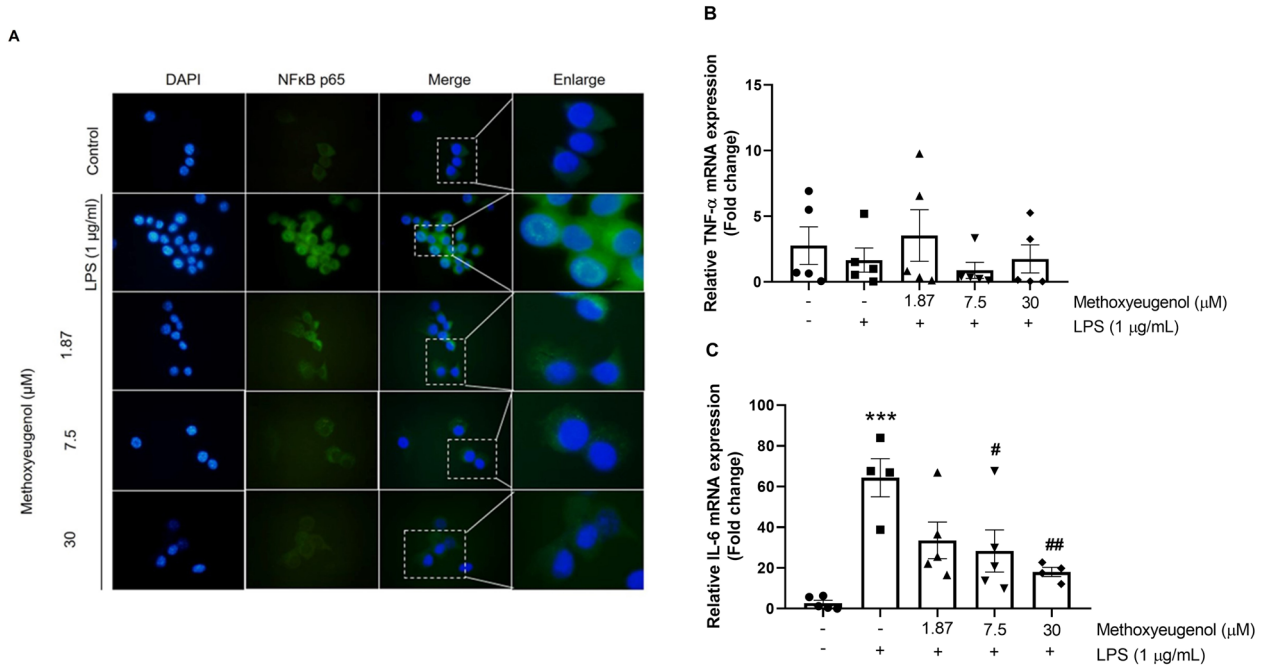


**Fig. 2** Effects of methoxyeugenol on NFκB p65 staining and in cytokine mRNA expression in RAW 264.7 cells. **A** Cells ( $1 \times 10^4$  cells/well in 8-chamber culture slides) were pretreated with methoxyeugenol (1.87–30  $\mu\text{M}$ ) for 1 h, exposed to LPS (1  $\mu\text{g/mL}$ ) for more than 1 h and stained with NFκB p65. **B, C** RAW 264.7 cells ( $2.5 \times 10^5$  cells/well in 6-well plates) were pretreated with methoxyeugenol (1.87–30  $\mu\text{M}$ ) for 1 h and exposed to LPS (1  $\mu\text{g/mL}$ ) for 16 h. The relative mRNA expression of **B** TNF- $\alpha$  and **C** IL-6 was assessed by RT-PCR. \*Significant difference relative to control; # significant difference relative to LPS (one-way ANOVA followed by Tukey's test) \* $p < 0.05$ , \*\* $p < 0.01$ , and \*\*\* $p < 0.001$ . Results are expressed as target gene/B2M, and data represent the mean  $\pm$  SEM from three independent experiments.

IL-1 $\beta$  release (Fig. 4F). Nevertheless, our data revealed that LPS-induced ALI led to an increase in the TNF- $\alpha$  and IL-6 levels, whereas treatment with methoxyeugenol promoted a reduction in the release of TNF- $\alpha$  and IL-6 (Fig. 4G, H). IL-10 levels in the LPS-induced ALI mice increased in comparison to the sham group; however, LPS-induced ALI mice pretreated with methoxyeugenol showed a decrease in IL-10 levels (Fig. 4I).

### Methoxyeugenol Decreases ROS Production in LPS-induced ALI Mice

Oxidative stress characterized by excessive ROS production is an important component in ALI. LPS-induced ALI mice had an increase in ROS production; however, the mice pretreated with methoxyeugenol had a decrease in the formation of ROS in the lung tissue (Fig. 5).

### Methoxyeugenol Suppresses the Formation of NETs in LPS-induced ALI Mice

Lastly, we investigated if treatment with methoxyeugenol was able to reduce the formation of NETs. Immunofluorescence was performed in the BAL cells to visualize the NETs colocalized with anti-MPO (1:250) (Cell Signaling Technology, USA); we observed that LPS-induced ALI mice had an increase in the formation of NETs when compared to the sham group (Fig. 6A). Nonetheless, mice pretreated with methoxyeugenol had a reduction in the formation of NETs (Fig. 6A). In addition, we also demonstrated the same result through scanning electron microscopy (Fig. 6B). The levels of extracellular DNA were measured in the BAL supernatants. LPS-induced ALI mice showed an increase in the DNA levels, while LPS-induced ALI mice pretreated with methoxyeugenol showed a reduction in the extracellular DNA levels (Fig. 6C), corroborating with results found

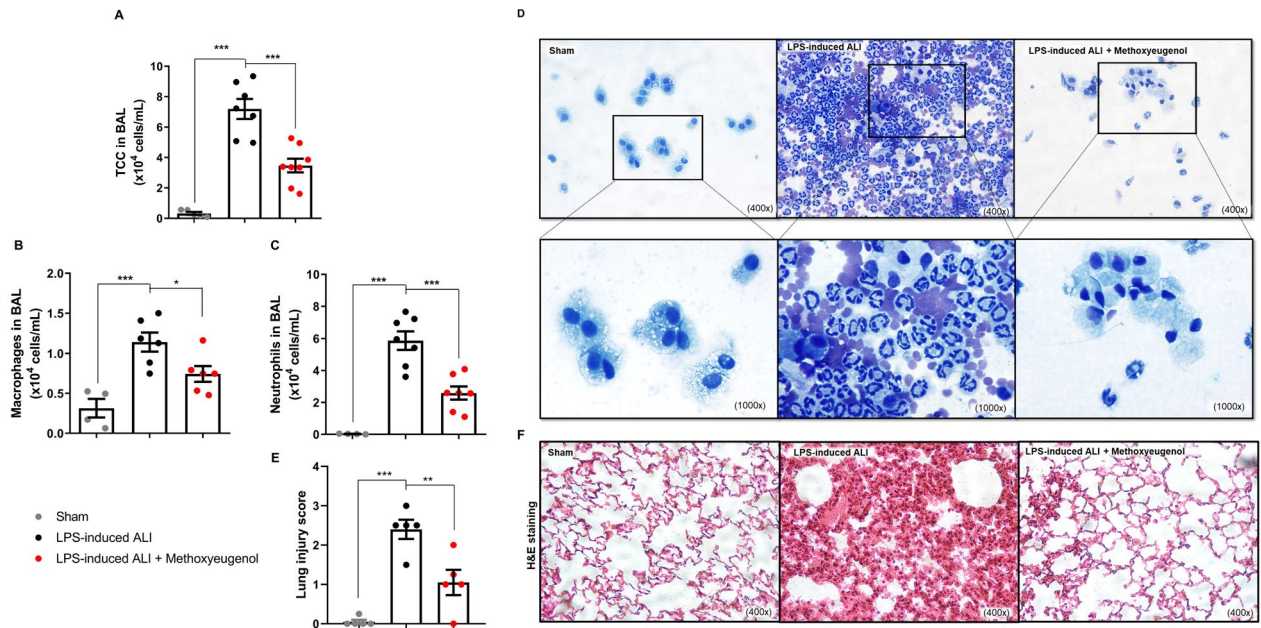


**Fig. 3** Methoxyeugenol reduces the influx of inflammatory cells into the lung of LPS-induced ALI mice. **A** Total cell counts (TCC), **B** macrophage counts, and **C** neutrophil counts in the BAL of mice. **D** Representative images of the differential cell count stained with H&E (400 $\times$  and 1000 $\times$  magnification). **E** Histopathological changes measured by injury score. **F** Representative lung sections stained with H&E (400 $\times$  magnification). Results are expressed as mean  $\pm$  SEM ( $n=6-8$ ). \* $p<0.05$ , \*\* $p<0.01$ , and \*\*\* $p<0.001$  (one-way ANOVA followed by Tukey's test).

in immunofluorescence and scanning electron microscopy. To exclude the possibility of extracellular DNA being derived from dead cells, we evaluated apoptosis and necrosis by flow cytometric analysis. Our results showed that the extracellular DNA observed was not due to cell death, since the cells remained viable in the studied groups (Fig. 6D, E).

## DISCUSSION

ALI, a severe pulmonary inflammatory disease, has limited treatment options and presents with high morbidity and mortality among patients [1]. We explored the effects of methoxyeugenol on ALI. Methoxyeugenol inhibited the proliferation of cells in a human endometrial adenocarcinoma cell line. The methoxyeugenol reduced the proliferative capacity of human endometrial adenocarcinoma cells by upregulating the expressions of p21 and p53 without changing  $\beta$ -galactosidase activity (SA- $\beta$ -gal), a cell senescence marker [15]. Furthermore, methoxyeugenol at 30  $\mu$ M decreased the proliferative rate and induced a quiescent phenotype in the hepatic stellate

cells. This same study demonstrated that methoxyeugenol at 0.25 mg/kg suppressed inflammation and fibrosis via regulation of the NF $\kappa$ B signaling pathway in a model of liver fibrosis [10]. Based on this previous research, we selected 1.87–30  $\mu$ M and 0.25 mg/kg of methoxyeugenol to assess its anti-inflammatory effects on ALI. In the present study, it is evident that methoxyeugenol showed anti-inflammatory activity in in vitro and in vivo models of ALI. Other studies using the phenolic compound octyl gallate have already shown anti-inflammatory activity in ALI [16]. However, to our knowledge, this is the first study to show that a phenolic compound protects against lung inflammation through NF $\kappa$ B signaling and suppresses the formation of NETs.

Initially, we explored the role of methoxyeugenol using the murine macrophage RAW 264.7 cell line that has been utilized in in vitro research to reproduce the inflammation observed in ALI [17, 18]. Regarding in vitro tests, we showed that methoxyeugenol reduced the proliferation of RAW 264.7 cells induced by LPS. Besides, previous studies reported that LPS induces RAW 264.7 cells to release several pro-inflammatory cytokines, including TNF- $\alpha$ , IL-1 $\beta$ , and IL-6 [19, 20]. These releases



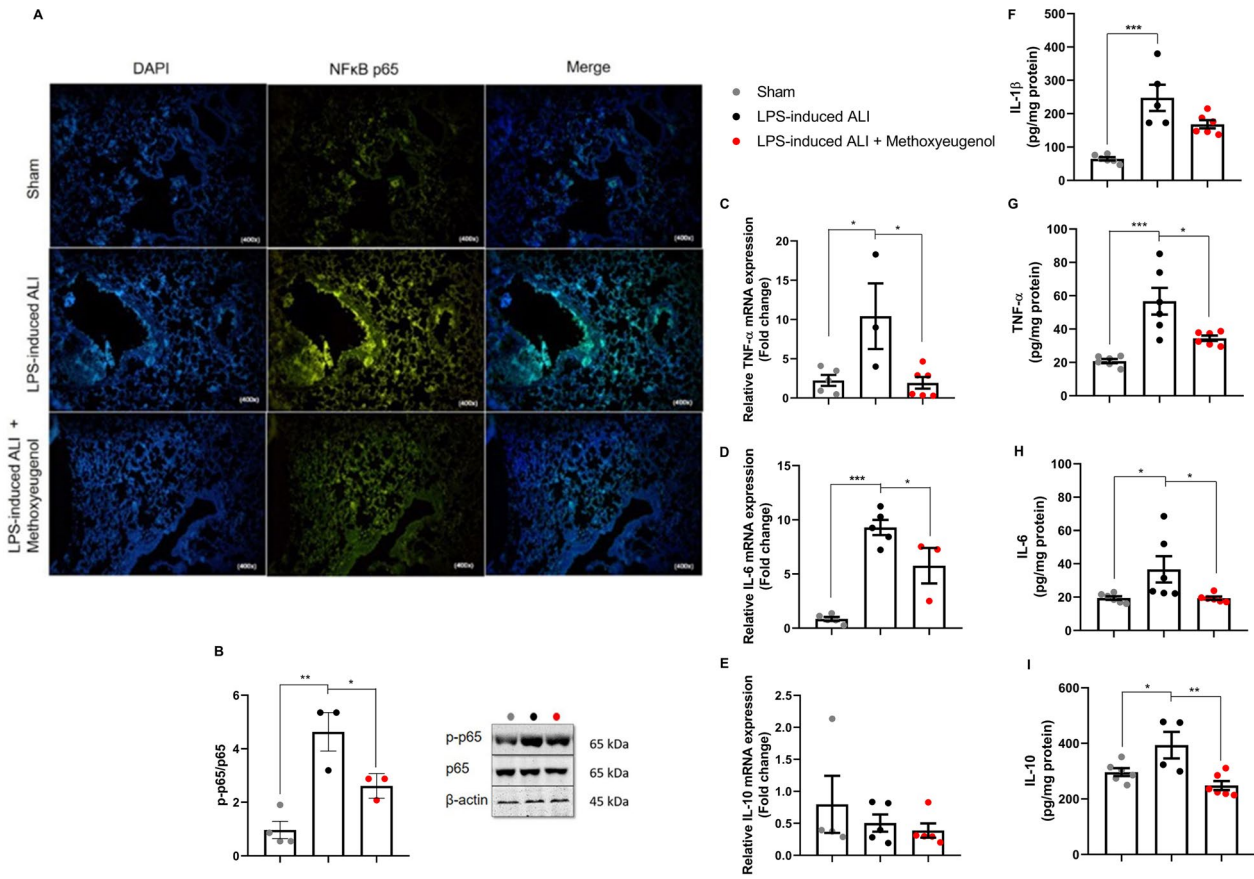


**Fig. 4** Methoxyeugenol suppresses the NFκB signaling pathway and decreases cytokine release in the lung of LPS-induced ALI mice. **A** Immunofluorescence of lung sections stained with a fluorescent NFκB p65 dye. **B** p65 and p-p65 protein expression in the lung tissues detected by Western blot. Relative gene expression (target gene/B2M) of **C** TNF-α, **D** IL-6, and **E** IL-10. Cytokine levels of **F** IL-1β, **G** TNF-α, **H** IL-6, and **I** IL-10 in the lung tissue. Results are expressed as mean ± SEM ( $n=4-8$ ). \* $p < 0.05$ , \*\* $p < 0.01$ , and \*\*\* $p < 0.001$  (one-way ANOVA followed by Tukey's test).

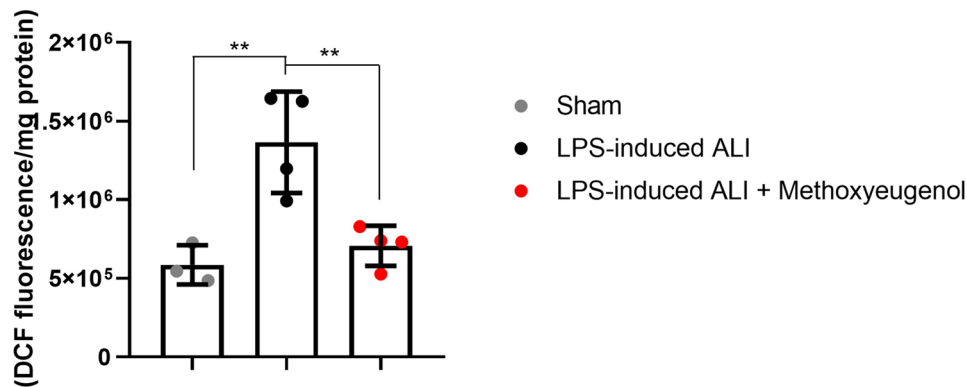


**Fig. 5** Methoxyeugenol decreases the ROS production in the lung tissue of LPS-induced ALI mice. Results are expressed as mean ± SEM ( $n=4$ ). \*\* $p < 0.01$  (one-way ANOVA followed by Tukey's test).

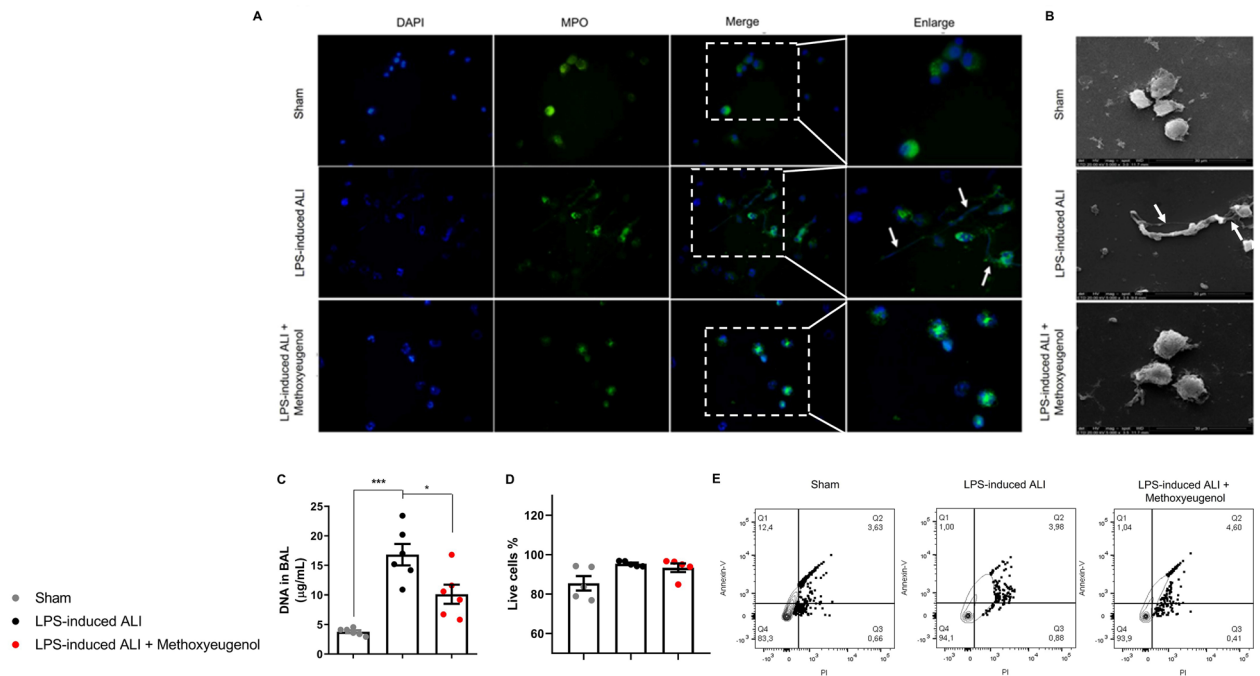


**Fig. 6** Methoxyeugenol protects against the formation of NETs in the lung tissue of LPS-induced ALI mice. **A** Cells ( $2 \times 10^5$ /mL) from BAL were plated in 8-chamber culture slides and incubated at  $37^\circ\text{C}$  with  $5\% \text{CO}_2$ . After 1 h of incubation, the cells were stimulated for another hour with PMA (50 nM), fixed (4% PFA), and marked-up with fluorescent dyes, MPO (green) and DAPI (blue). Arrows indicate the presence of the formation of NETs. **B** Cells ( $2 \times 10^5$ /mL) from BAL were plated in 8-chamber culture slides and incubated at  $37^\circ\text{C}$  with  $5\% \text{CO}_2$ . After 1 h of incubation, the cells were stimulated for another hour with PMA (50 nM) fixed with 2.5% glutaraldehyde. The samples were postfixed with 2% osmium tetroxide solution, followed by dehydration in graded acetone. The  $\text{CO}_2$  was used to execute the critical point technique and then mounting on a metallic support using carbon tape was performed. Gold was used to cover all samples, and images were captured by Inspect F50 (FEI, Oregon, EUA). **B** Quantification of extracellular DNA traps in the BAL supernatant. **C** Analysis of cell death in the BAL cells by annexin V (x-axis) and PI (y-axis). Results are expressed as a percentage of live cells. **D** Representative flow cytometric plots of studied groups. A total of 10,000 events were collected and results are expressed as mean  $\pm$  SEM ( $n=6$ ). \* $p < 0.05$  and \*\*\* $p < 0.001$  (one-way ANOVA followed by Tukey's test).

of inflammatory mediators have crucial roles in inflammatory diseases, such as ALI [2]. We performed an investigation to study the effect of methoxyeugenol on the mRNA expression of TNF- $\alpha$  and IL-6. No significant difference in the mRNA expression of TNF- $\alpha$  was found between the groups studied. A possible explanation is related to the sample collection time (16 h after stimulation with LPS), since TNF- $\alpha$  release can reach peak levels the first several hours after the inflammatory stimulus [21]. Nonetheless, a reduction in the mRNA expression of IL-6 was found. These in vitro results showed that methoxyeugenol has an anti-inflammatory effect against LPS-activated macrophages.

To reproduce the major lung inflammation features of ALI, LPS was administered intranasally in mice. Cell counts and histopathological examination revealed a great influx of inflammatory cells, alveolar rupture, and

pulmonary hemorrhage into the lungs of LPS-induced ALI mice, evidencing the success of induction of the ALI model. We found an increase in the macrophage counts. However, it was significantly reduced in mice pretreated with methoxyeugenol, which is in agreement with our in vitro findings. Although macrophages initiate the inflammatory process in ALI, the neutrophil influx is the hallmark of patients with ALI [1, 22]. In our study, we demonstrated that pretreatment with methoxyeugenol reduced the number of neutrophils, evidencing that methoxyeugenol has an important anti-inflammatory function in LPS-induced ALI mice.

In unstimulated cells, NF $\kappa$ B exists in the cytoplasm and binds to its inhibitory protein I $\kappa$ B. When the cells are stimulated by molecules, it leads to an interaction with the IKK complex, which then leads to the phosphorylation of I $\kappa$ B, and therefore results in I $\kappa$ B ubiquitination

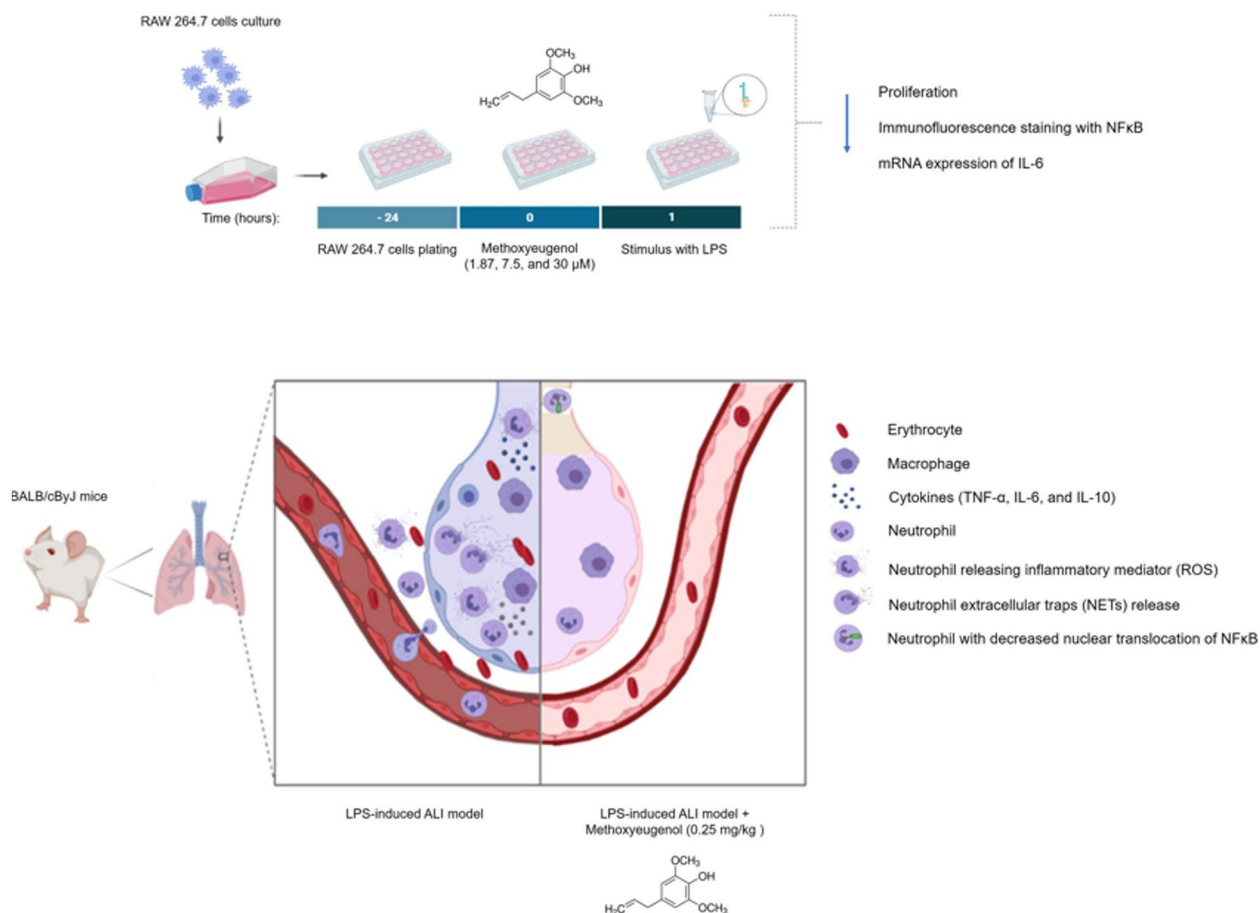


**Fig. 7** Summary of the effects of methoxyeugenol that lead to protection against inflammation in ALI. IL interleukin, LPS lipopolysaccharide, NET neutrophil extracellular trap, NF $\kappa$ B nuclear factor kappa B, ROS reactive oxygen species, and TNF- $\alpha$  tumor necrosis factor alpha.

and degradation. Once I $\kappa$ B is degraded, the phosphorylated p65 subunits translocate to the nucleus and induce the transcription of inflammatory mediators [23]. LPS is known to activate the NF $\kappa$ B signaling pathway. Macrophages recognize the LPS via Toll-like receptor 4 (TLR4), and cell signaling via TLR4 culminates in the activation of the NF $\kappa$ B pathway [24].

RAW 264.7 cells and the lung sections stained for NF $\kappa$ B p65 by immunofluorescence indicated that methoxyeugenol promotes a decrease in NF $\kappa$ B p65 nuclear translocation. According to the immunofluorescence results, we demonstrated that pretreatment with methoxyeugenol showed a decrease in the relative expression of p-p65/p65 analyzed by Western blot. Our data shows that methoxyeugenol prevents macrophage proliferation, suppressing activation of the NF $\kappa$ B pathway, which is responsible for transcriptional induction of cytokines.

The levels of cytokines in the lung tissue of mice were explored. IL-1 $\beta$  increases the permeability of pulmonary epithelium and induces lung tissue damage [25]. The release of IL-1 $\beta$  increased in the lung tissue of mice submitted to the ALI model. However, we did not find a significant decrease in the mice that received pretreatment with methoxyeugenol. The persistent increase of IL-6 and TNF- $\alpha$  levels are associated with the outcome of death in patients with ALI and with neutrophil recruitment [4, 26]. We investigated the levels of the pro-inflammatory cytokines IL-6 and TNF- $\alpha$ , and the reduction of these cytokine levels was found in the group pretreated with methoxyeugenol. These findings prove that the anti-inflammatory effects of methoxyeugenol involve the suppression of the NF $\kappa$ B signaling pathway, which results in the decreased release of pro-inflammatory cytokines. Furthermore, although we found no difference in IL-10

mRNA expression, a decrease in the IL-10 protein levels in the lung tissue of the group pretreated with methoxyeugenol was evident. Even though IL-10 is an anti-inflammatory cytokine, its production can be increased in several diseases, such as ALI and sepsis [27].

Lung damage is mediated, in part, by increased levels of ROS, which damage nucleic acids, lipids, and proteins [28]. The high generation of ROS observed in the LPS-induced ALI mice was decreased in mice that received pretreatment with methoxyeugenol, showing that methoxyeugenol induces protection against the cellular injury induced by ROS. Our data has been corroborated by a study, which shows that methoxyeugenol has antioxidant properties, even when maintained under high oxidative stress conditions, as those produced by carbon tetrachloride (CCl<sub>4</sub>) [10]. It is known that the high production of ROS can be essential to the formation of NETs. NETs are formed by DNA and intact neutrophilic granules, such as MPO, and were initially described as a new mechanism to catch, immobilize, and potentially kill bacteria [29]. Subsequently, it was reported that, although the release of NETs has a beneficial effect against infectious agents, excessive production could have a deleterious role in several diseases [30, 31]. The biomarkers of NETs in the serum of patients with transfusion-related acute lung injury (TRALI) were found. Moreover, the abundant formation of NETs in the alveoli of an experimental mice model of TRALI and patients with TRALI were observed [32]. A study using a mice model of ventilator-induced lung injury demonstrated that NETs lead to compromise of ventilation and pulmonary microcirculation [33]. Furthermore, in the experimental model of TRALI, it was revealed that the degradation of NET-derived structures by DNase decreased the severity of lung injury and mortality of the mice [34], showing an interesting approach.

We provide evidence that neutrophils recruited to the lungs during ALI induced by LPS promote the formation of NETs. We showed the colocalization of extracellular DNA with MPO in BAL neutrophils through immunofluorescence microscopy analysis. Interestingly, our data show that pretreatment with methoxyeugenol promotes a reduction in the formation of NETs. These findings observed in the immunofluorescence microscopy analysis are consistent with experiments using scanning electron microscopy. NETs have also been reported as a process of cell death, called NETosis, which results in permeabilization of both plasma and nuclear membranes, releasing nuclear DNA [35]. Although some studies show that the release of extracellular DNA traps is dependent

on death [29], other studies provide evidence that cells are viable [36, 37]. We evaluated whether the DNA extracellular released by neutrophils was derived from dead cells. In our study, we confirmed that the release of NETs was not due to cell death, since the cells remained viable in the studied groups.

Based on these in vitro and in vivo findings, we provided evidence that methoxyeugenol had powerful anti-inflammatory activity. The LPS-stimulated RAW 264.7 cells pretreated with methoxyeugenol (7.5 and 30  $\mu$ M) remarkably reduced the proliferation and mRNA expression of IL-6. In LPS-induced ALI mice, methoxyeugenol exhibited a significant protective effect, based on influx reduction of macrophages and neutrophils into the lungs; reduction in the release of cytokines IL-6, TNF- $\alpha$ , and IL-10; and reduction in reactive oxygen species (ROS) formation. We showed that the anti-inflammatory effects of methoxyeugenol are associated with the suppression of the NF $\kappa$ B signaling pathway. Furthermore, to our knowledge, we showed for the first time that a phenolic compound, from a synthetic source, protects against lung inflammation and promotes a reduction in the formation of NETs. To summarize our data, Fig. 7 shows the effects of methoxyeugenol on LPS-stimulated RAW 264.7 cells and LPS-induced ALI mice. These findings provided evidence for the use of methoxyeugenol as a new strategy to control lung inflammation and suppress the formation of NETs in ALI.

## AUTHOR CONTRIBUTIONS

GLA and JRO designed the research. GLA, LSM, BPC, BSB, and VGSL conducted all experiments. KHA conducted the experiment with flow cytometry. ZSMCF supported the experiment with the MagPix assay. GLA wrote the manuscript, which was revised for intellectual content by BPC, LSM, and JRO. The authors read and approved the final manuscript.

## FUNDING

This study was financed, in part, by the Coordenação de Aperfeiçoamento de Pessoal de Nível Superior (CAPES), Brazil (Finance Code 001).

## AVAILABILITY OF DATA AND MATERIAL

Data and material will be provided by the authors if requested.

## DECLARATIONS



**Consent for Publication** Not applicable.

**Animal Ethics** All experiments were performed following the National Institutes of Health Guide for the Care and Use of Laboratory Animals. The study and all experiments were approved by the Animal Ethics Committee from the PUCRS with registration number 9607.

**Conflict of Interest** The authors declare no conflicts of interest.

## REFERENCES

- Fanelli, V., and V.M. Ranieri. 2015. Mechanisms and clinical consequences of acute lung injury. *Annals of the American Thoracic Society* 12 (Suppl 1): S3-8.
- Mowery, N.T., W.T.H. Terzian, and A.C. Nelson. 2020. Acute lung injury. *Current Problems in Surgery* 57: 100-777.
- Dhaliwal, K., E. Scholefield, D. Ferenbach, M. Gibbons, R. Duffin, D.A. Dorward, A.C. Morris, D. Humphries, A. MacKinnon, T.S. Wilkinson, et al. 2012. Monocytes control second-phase neutrophil emigration in established lipopolysaccharide-induced murine lung injury. *American Journal of Respiratory and Critical Care Medicine* 186: 514-524.
- Levitt, J.E., M.K. Gould, L.B. Ware, and M.A. Matthay. 2009. Analytic review: The pathogenetic and prognostic value of biologic markers in acute lung injury. 24: 151-167.
- Liu, S., X. Su, P. Pan, L. Zhang, Y. Hu, H. Tan, D. Wu, B. Liu, H. Li, H. Li, et al. 2016. Neutrophil extracellular traps are indirectly triggered by lipopolysaccharide and contribute to acute lung injury. *Science and Reports* 6: 37252.
- Hamaguchi, S., T. Hirose, N. Matsumoto, Y. Akeda, T. Irisawa, M. Seki, H. Hosotsubo, K. Yamamoto, O. Tasaki, K. Oishi, et al. 2014. Neutrophil extracellular traps in bronchial aspirates: A quantitative analysis. *European Respiratory Journal* 43: 1709-1718.
- López, V., J. Gerique, E. Langa, C. Berzosa, M.S. Valero, and C. Gómez-Rincón. 2015. Anthelmintic effects of nutmeg (*Myristica fragrans*) on *Anisakis simplex* L3 larvae obtained from *Micromesistius potassou*. *Research in Veterinary Science* 100: 148-152.
- Agnihotri, S., S. Wakode, and M. Ali. 2012. Essential oil of *Myrica esculenta* Buch. Ham.: composition, antimicrobial and topical anti-inflammatory activities. *Natural Product Research* 26: 2266-2269.
- Paul, S., J.K. Hwang, H.Y. Kim, W.K. Jeon, C. Chung, and J.S. Han. 2013. Multiple biological properties of macelignan and its pharmacological implications. *Archives of Pharmacol Research* 36: 264-272.
- de Souza, Basso B., G.V. Haute, M. Ortega-Ribera, C. Luft, G.L. Antunes, M.S. Bastos, L.P. Carlessi, V.G. Levorse, E. Cassel, M.V. Fagundes Donadio, et al. 2021. Methoxyeugenol deactivates hepatic stellate cells and attenuates liver fibrosis and inflammation through a PPAR- $\gamma$  and NF- $\kappa$ B mechanism. *Journal of Ethnopharmacology* 280: 114433.
- Antunes, G.L., J.S. Silveira, D.B. Kaiber, C. Luft, M.S. da Costa, E.P. Marques, F.S. Ferreira, R.V. Breda, A.T.S. Wyse, R.T. Stein, et al. 2020. Cholinergic anti-inflammatory pathway confers airway protection against oxidative damage and attenuates inflammation in an allergic asthma model. *Journal of Cellular Physiology* 235: 1838-1849.
- Zhang, Z., Z., Luo, A., Bi, W., Yang, W., An, X., Dong, R., Chen, S., Yang, H., Tang, X.J., Han, and Ejop. 2017. Compound edaravone alleviates lipopolysaccharide (LPS)-induced acute lung injury in mice. *European Journal of Pharmacology*. 811: 1-11.
- LeBel, C.P., H. Ischiropoulos, and S.C. Bondy. 1992. Evaluation of the probe 2',7'-dichlorofluorescein as an indicator of reactive oxygen species formation and oxidative stress. *Chemical Research in Toxicology* 5: 227-231.
- Additives and Products or Substances used in Animal Feed. 2021 Available online: <https://www.efsa.europa.eu/sites/default/files/wgs/feed-additives/wg-feed-flavourings-2018-2021.pdf>
- Costa, B.P., M.T. Nassr, F.M. Diz, K.H.A. Fernandes, G.L. Antunes, L.K. Grun, F.M. Barbé-Tuana, F.B. Nunes, G. Branchini, and J.R. de Oliveira. 2021. Methoxyeugenol regulates the p53/p21 pathway and suppresses human endometrial cancer cell proliferation. *Journal of Ethnopharmacology* 267: 113645.
- Haute, G.V., C. Luft, G.L. Antunes, J.S. Silveira, Basso B. de Souza, M.S. da Costa, V.G.S. Levorse, D.B. Kaiber, and M.V.F. Donadio. 2020. *Gracia-Sancho JJocp: Anti-inflammatory effect of octyl gallate in alveolar macrophages cells and mice with acute lung injury*. 235: 6073-6084.
- Li, L., S. Zhang, Y. Xin, J. Sun, F. Xie, L. Yang, Z. Chen, H. Chen, F. Liu, Y. Xuan, and Z. You. 2018. Role of Quzhou Fructus Aurantii Extract in Preventing and Treating Acute Lung Injury and Inflammation. *Scientific Reports* 8: 1698.
- Tong, Y., Z. Yu, Z. Chen, R. Zhang, X. Ding, X. Yang, X. Niu, M. Li, L. Zhang, T.R. Billiar, et al. 2021. The HIV protease inhibitor Saquinavir attenuates sepsis-induced acute lung injury and promotes M2 macrophage polarization via targeting matrix metalloproteinase-9. *Cell Death & Disease* 12: 67.
- Xie, X., S. Sun, W. Zhong, L.W. Soromou, X. Zhou, M. Wei, Y. Ren, and Y. Ding. 2014. Zingerone attenuates lipopolysaccharide-induced acute lung injury in mice. *International Immunopharmacology* 19: 103-109.
- Qin, X., X. Jiang, X. Jiang, Y. Wang, Z. Miao, W. He, G. Yang, Z. Lv, Y. Yu, and Y. Zheng. 2016. Micheliolide inhibits LPS-induced inflammatory response and protects mice from LPS challenge. *Science and Reports* 6: 23240.
- Rodgers, K.R., Y. Lin, T.J. Langan, Y. Iwakura, and R.C. Chou. 2020. Innate immune functions of astrocytes are dependent upon tumor necrosis factor-alpha. *Scientific Reports* 10: 7047.
- Zemans, R.L., S.P. Colgan, and G.P. Downey. 2009. Trans-epithelial migration of neutrophils: Mechanisms and implications for acute lung injury. *American Journal of Respiratory Cell and Molecular Biology* 40: 519-535.
- Liu, T., L. Zhang, D. Joo, and S.-C. Sun. 2017. NF- $\kappa$ B signaling in inflammation. *Signal Transduction and Targeted Therapy* 2: 17023.
- Dorrington, M.G., and I.D. Fraser. 2019. NF- $\kappa$ B signaling in macrophages: dynamics, crosstalk, and signal integration. *Frontiers in Immunology* 10: 705.
- Ju, M., B. Liu, H. He, Z. Gu, Y. Liu, Y. Su, D. Zhu, J. Cang, and Z. Luo. 2018. MicroRNA-27a alleviates LPS-induced acute lung injury in mice via inhibiting inflammation and apoptosis through modulating TLR4/MyD88/NF- $\kappa$ B pathway. *Cell Cycle* 17: 2001-2018.
- Parsons, P.E., M.D. Eisner, B.T. Thompson, M.A. Matthay, M. Ancukiewicz, G.R. Bernard, and A.P. Wheeler. 2005. Lower tidal volume ventilation and plasma cytokine markers of inflammation

- in patients with acute lung injury. *Critical Care Medicine* 33: 1–6; discussion 230–232.
27. Li, X., Z. Xu, X. Pang, Y. Huang, B. Yang, Y. Yang, K. Chen, X. Liu, P. Mao, and Y. Li. 2017. Interleukin-10/lymphocyte ratio predicts mortality in severe septic patients. *Plos One* 12: e0179050.
  28. Haider, L., M.T. Fischer, J.M. Frischer, J. Bauer, R. Höftberger, G. Botond, H. Esterbauer, C.J. Binder, J.L. Witztum, and H. Lassmann. 2011. Oxidative damage in multiple sclerosis lesions. *Brain* 134: 1914–1924.
  29. Brinkmann, V., U. Reichard, C. Goosmann, B. Fauler, Y. Uhlemann, D.S. Weiss, Y. Weinrauch, and A. Zychlinsky. 2004. Neutrophil extracellular traps kill bacteria. *Science* 303: 1532–1535.
  30. Zuo, Y., S. Yalavarthi, H. Shi, K. Gockman, M. Zuo, J.A. Madison, C. Blair, A. Weber, B.J. Barnes, M. Egeblad, et al. 2020. Neutrophil extracellular traps in COVID-19. *JCI Insight*, 5.
  31. Silveira, J.S., G.L. Antunes, D.B. Kaiber, M.S. da Costa, E.P. Marques, F.S. Ferreira, R.B. Gassen, R.V. Breda, A.T.S. Wyse, P. Pitrez, and A.A. da Cunha. 2019. Reactive oxygen species are involved in eosinophil extracellular traps release and in airway inflammation in asthma. *Journal of Cellular Physiology* 234: 23633–23646.
  32. Thomas, G.M., C. Carbo, B.R. Curtis, K. Martinod, I.B. Mazo, D. Schatzberg, S.M. Cifuni, T.A. Fuchs, U.H. von Andrian, J.H. Hartwig, et al. 2012. Extracellular DNA traps are associated with the pathogenesis of TRALI in humans and mice. *Blood* 119: 6335–6343.
  33. Rossaint, J., J.M. Herter, H. Van Aken, M. Napirei, Y. Döring, C. Weber, O. Soehnlein, and A. Zarbock. 2014. Synchronized integrin engagement and chemokine activation is crucial in neutrophil extracellular trap-mediated sterile inflammation. *Blood* 123: 2573–2584.
  34. Abrams, S.T., N. Zhang, J. Manson, T. Liu, C. Dart, F. Baluwa, S.S. Wang, K. Brohi, A. Kipar, W. Yu, et al. 2013. Circulating histones are mediators of trauma-associated lung injury. *American Journal of Respiratory and Critical Care Medicine* 187: 160–169.
  35. Fuchs, T.A., U. Abed, C. Goosmann, R. Hurwitz, I. Schulze, V. Wahn, Y. Weinrauch, and V. Brinkmann. 2007. *Zychlinsky AJT-Job: Novel cell death program leads to neutrophil extracellular traps*. 176: 231–241.
  36. Yousefi, S., J.A. Gold, N. Andina, J.J. Lee, A.M. Kelly, E. Kozlowski, I. Schmid, A. Straumann, J. Reichenbach, G.J. Gleich, and H.U. Simon. 2008. Catapult-like release of mitochondrial DNA by eosinophils contributes to antibacterial defense. *Nature Medicine* 14: 949–953.
  37. Cunha, A.A., B.N. Porto, N.K. Nuñez, R.G. Souza, M.H. Vargas, J.S. Silveira, T.T. Souza, N. Jaeger, and P.M. Pitrez. 2014. Extracellular DNA traps in bronchoalveolar fluid from a murine eosinophilic pulmonary response. *Allergy* 69: 1696–1700.

**Publisher's Note** Springer Nature remains neutral with regard to jurisdictional claims in published maps and institutional affiliations.